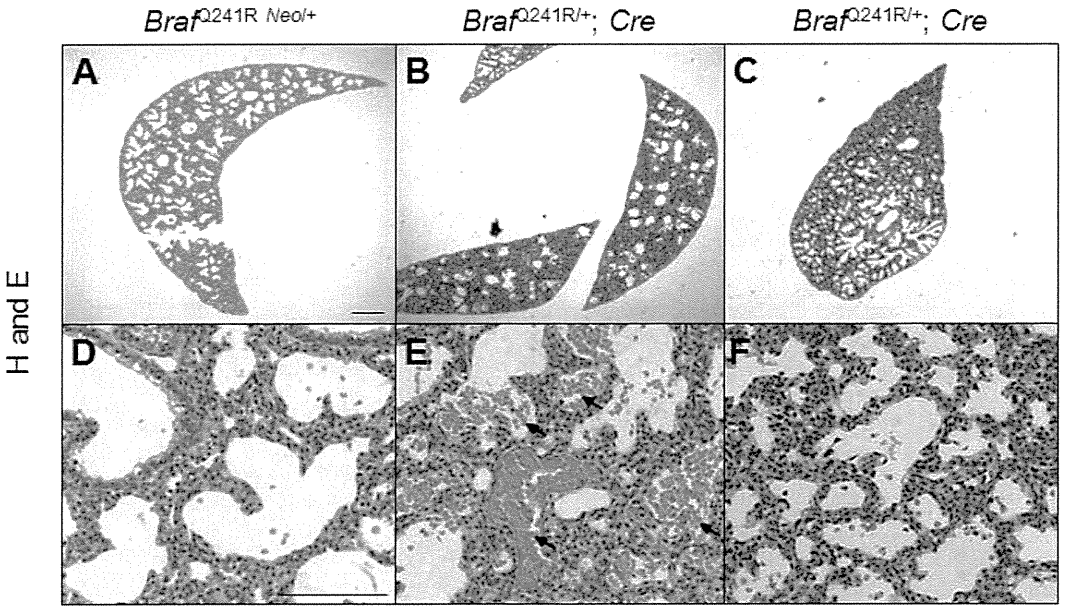

Supplementary Figure 3 Histological analysis of lung. Lung sections of *Braf*$^{Q241R\ Neo/+}$ and *Braf*$^{Q241R/+}$; *Cre* embryos at E18.5 were stained with H&E. The arrows indicate alveolar hemorrhage. Lower panels show higher-magnification views of lung. Scale bars in upper panels = 200 μm and those in lower panels = 100 μm.

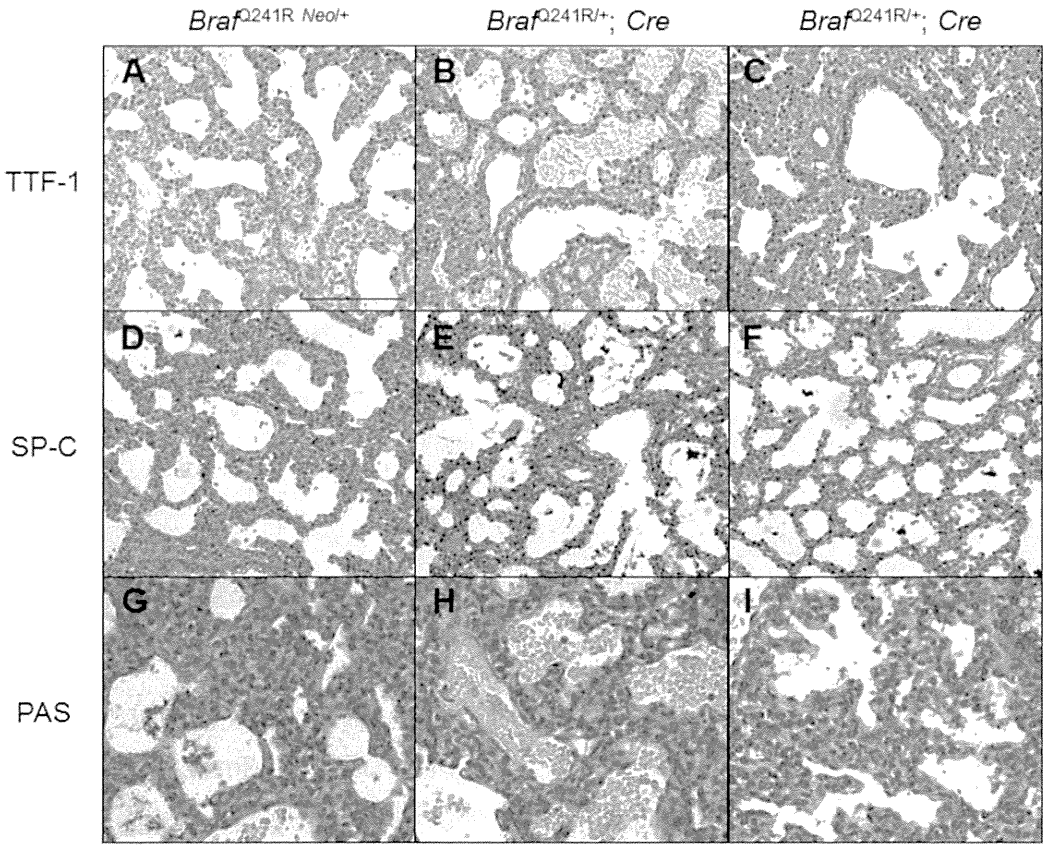

Supplementary Figure 4 Assessment of lung maturation in *Braf*$^{Q241R/+}$; *Cre* embryos. Sections of lungs from *Braf*$^{Q241R\ Neo/+}$ and *Braf*$^{Q241R/+}$; *Cre* embryos at E18.5 were stained with antibodies against TTF-1 (**A-C**), pro-SP-C (**D-F**) and periodic acid-schiff (PAS, **G-I**). Scale bars = 100 μm.

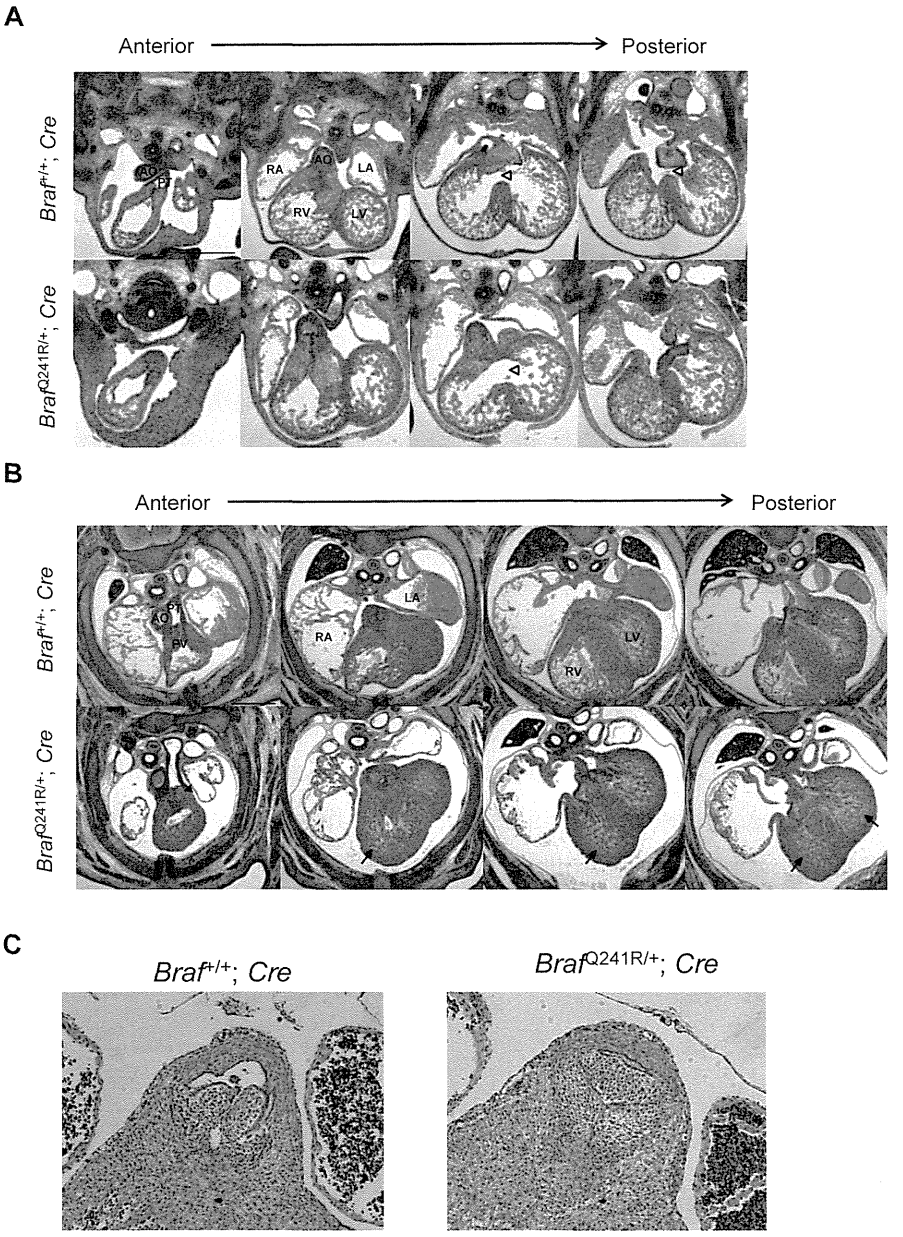

Supplementary Figure 5 Cardiac phenotype of *Braf*$^{Q241R/+}$; *Cre* embryos at E12.5 and E14.5. (**A-C**) Sequential anterior to posterior sections of embryonic hearts from *Braf*$^{+/+}$; *Cre* and *Braf*$^{Q241R/+}$; *Cre* at E12.5 (**A**) and E14.5 (**B**) stained with H&E. Ventricular septal defect (VSD, open arrowheads), enlarged pulmonary valve (solid arrowhead) and abnormal hypertrabeculation (arrows) are shown. (**C**) Representative of the enlarged pulmonary valves in *Braf*$^{Q241R/+}$; *Cre* embryos at E14.5. LV, left ventricle; RV, right ventricle; LA, left atrium; RA, right atrium; PT, pulmonary trunk; PV, pulmonary valve; AO, aorta. Scale bars = 500 μm.

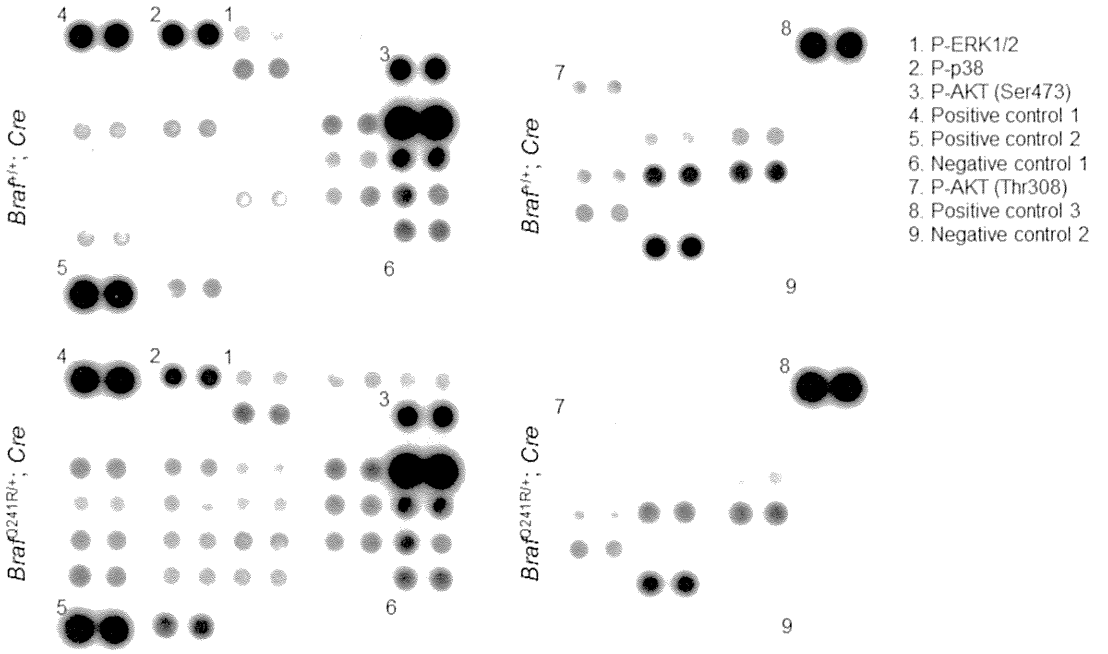

Supplementary Figure 6 Changes in phosphorylation level of kinase proteins in *Braf*$^{Q241R/+}$; *Cre* embryos. Protein extracts of embryonic hearts from embryos at E16.5 were subjected to Phospho-Kinase Antibody Array. Each phosphorylated protein displays duplicate signal spots, as well as three internal controls and two negative controls.

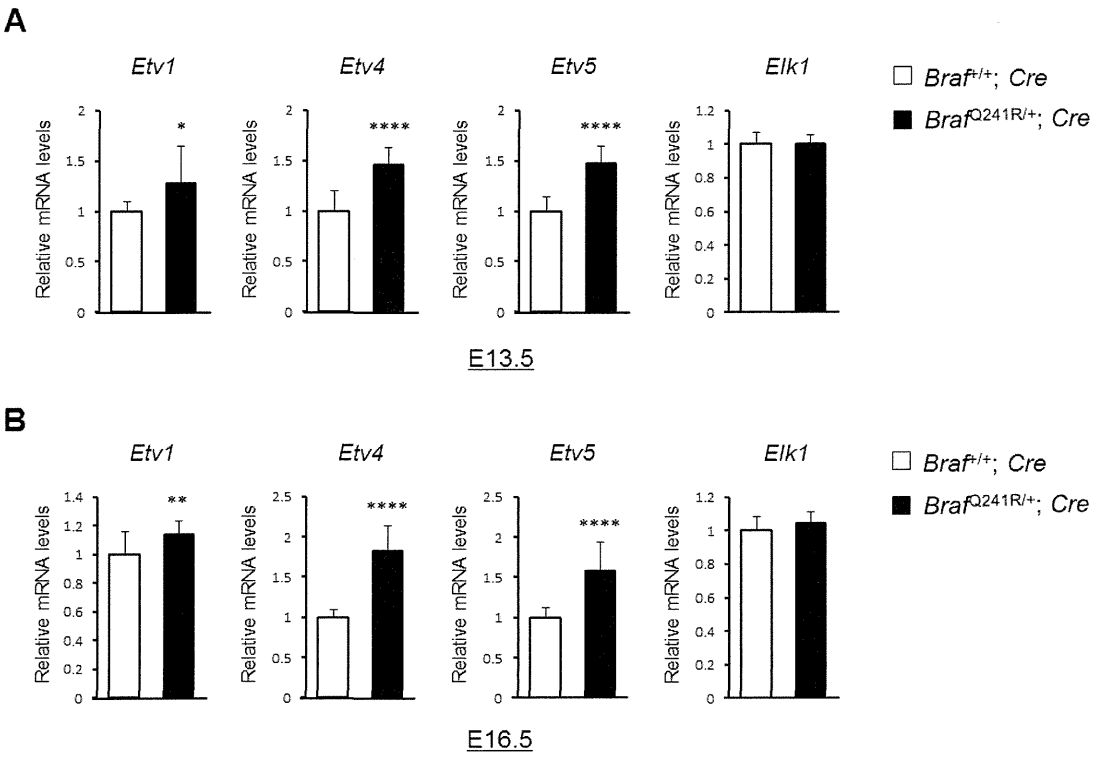

Supplementary Figure 7 Changes in expression level of Ets transcription factors in *Braf*$^{Q241R/+}$; *Cre* embryo hearts at E13.5 and E16.5. (**A,B**) Cardiac mRNA levels were determined by quantitative reverse transcription-PCR. mRNA levels were normalized by those of *Gapdh*, and those in *Braf*$^{+/+}$; *Cre* are set at 1. Data are the means ± S.D. At E13.5; *Braf*$^{+/+}$; *Cre* (*n* = 11) and *Braf*$^{Q241R/+}$; *Cre* (*n* = 11), At E16.5; *Braf*$^{+/+}$; *Cre* (*n* = 10) and *Braf*$^{Q241R/+}$; *Cre* (*n* = 14). *, $P<0.05$, **, $P<0.01$, ****, $P<0.0001$ vs. *Braf*$^{+/+}$; *Cre*. *Etv1*, *Etv4* and *Etv5* encode ER81, Pea3 and ERM, respectively.

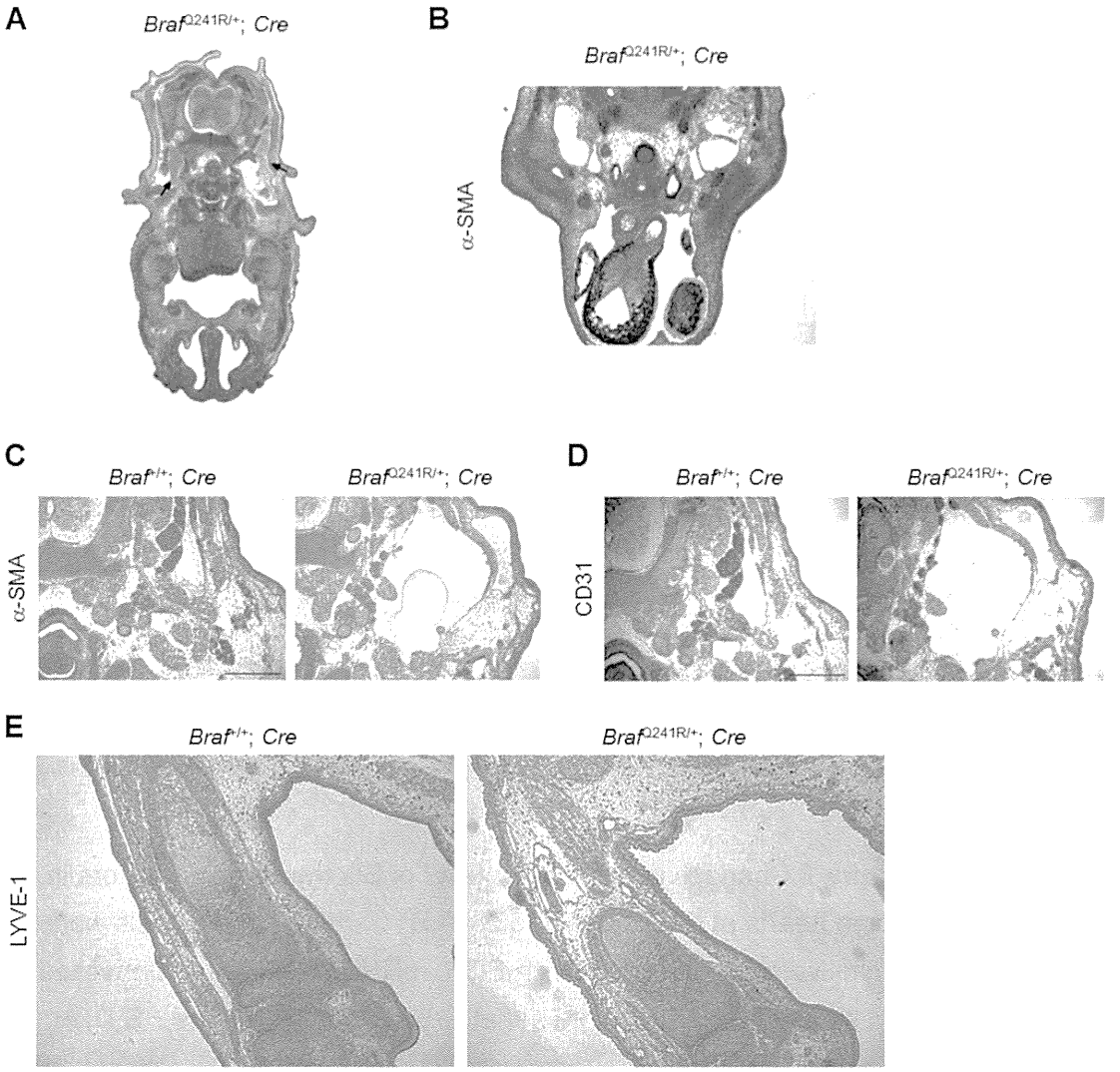

Supplementary Figure 8 Lymphatic vessel development of *Braf*$^{Q241R/+}$; *Cre* embryos. (**A**) H&E staining of transverse sections of *Braf*$^{+/+}$; *Cre* and *Braf*$^{Q241R/+}$; *Cre* embryos at E16.5. The arrows indicate blood cells in jugular lymph sac. (**B-E**) Sections of *Braf*$^{+/+}$; *Cre* and *Braf*$^{Q241R/+}$; *Cre* embryos at E12.5 (**B**), E16.5 (**C,D**) and E18.5 (**E**) were stained with antibodies against α-SMA, CD31 or LYVE-1. Jugular lymph sac was negative for α-SMA and CD31 in both *Braf*$^{+/+}$; *Cre* and *Braf*$^{Q241R/+}$; *Cre* embryos (**B-D**). Distended subcutaneous lymphatic vessels were observed in *Braf*$^{+/+}$; *Cre* and *Braf*$^{Q241R/+}$; *Cre* embryos (**E**). Scale bars = 500 μm (**C,D**).

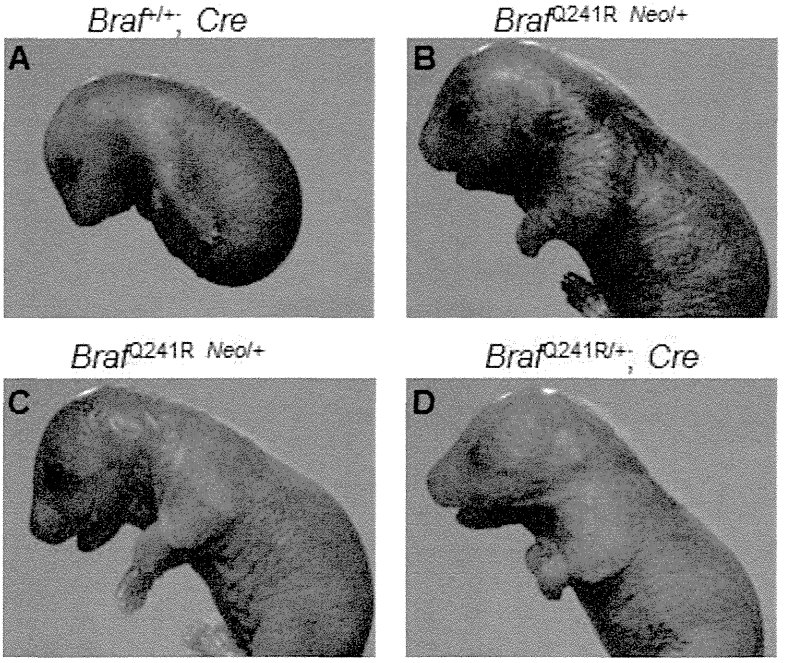

Supplementary Figure 9 Teratogenic effects of PD0325901 treatment in *Braf*$^{+/+}$; *Cre* and *Braf*$^{Q241R\ Neo/+}$ mice at P0. (**A-C**) PD0325901-treated (1.0 mg/kg) *Braf*$^{+/+}$; *Cre* and *Braf*$^{Q241R\ Neo/+}$ mice at P0 showed congenital anomaly (**A**), craniofacial abnormalities (**B**) and open eyes (**B,C**). PD0325901-treated (1.0 mg/kg) *Braf*$^{Q241R/+}$; *Cre* mice appeared normal (**D**).

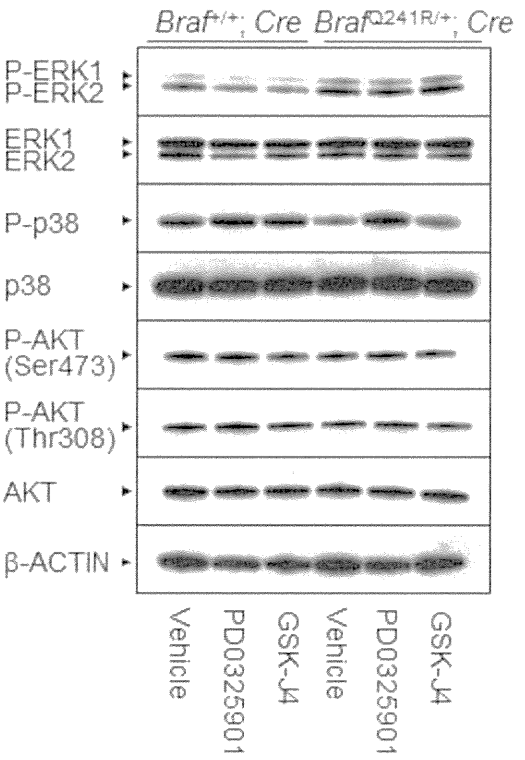

Supplementary Figure 10 Influence of treatment with PD0325901 or GSK-J4 on the cardiac signaling of *Braf*$^{Q241R/+}$; *Cre* embryos. Western blotting of the hearts from *Braf*$^{+/+}$; *Cre* and *Braf*$^{Q241R/+}$; *Cre* embryos at E16.5 (vehicle-treated pooled samples; *Braf*$^{+/+}$; *Cre* (*n* = 8), *Braf*$^{Q241R/+}$; *Cre* (*n* = 8). PD0325901-treated pooled samples; *Braf*$^{+/+}$; *Cre* (*n* = 6), *Braf*$^{Q241R/+}$; *Cre* (*n* = 7)). GSK-J4-treated pooled samples; *Braf*$^{+/+}$; *Cre* (*n* = 8), *Braf*$^{Q241R/+}$; *Cre* (*n* = 7)). β-ACTIN is shown as a loading control. The arrowheads indicate the bands corresponding to each protein.

Supplementary Table 1

Protein levels of the MAPK pathways and PI3K/AKT pathway in *Braf*$^{Q241R/+}$; *Cre* embryos

	E12.5		E14.5	
	Braf$^{+/+}$; *Cre* (*n* =5)	*Braf*$^{Q241R/+}$; *Cre* (*n* =5)	*Braf*$^{+/+}$; *Cre* (*n* =4)	*Braf*$^{Q241R/+}$; *Cre* (*n* =5)
BRAF	1.00 ± 0.15	0.79 ± 0.15	1.00 ± 0.06	1.03 ± 0.11
CRAF	1.00 ± 0.06	0.96 ± 0.15	1.00 ± 0.06	1.03 ± 0.09
MEK	1.00 ± 0.15	1.18 ± 0.26	1.00 ± 0.12	0.72 ± 0.28
P-MEK	1.00 ± 0.35	1.00 ± 0.53	1.00 ± 0.18	1.77 ± 0.95
ERK1/2	1.00 ± 0.04	1.01 ± 0.08	1.00 ± 0.09	0.95 ± 0.05
P-ERK1/2	1.00 ± 0.19	1.10 ± 0.25	1.00 ± 0.23	1.29 ± 0.18
p38	1.00 ± 0.02	0.93 ± 0.13	1.00 ± 0.06	1.05 ± 0.08
P-p38	1.00 ± 0.11	0.84 ± 0.11	1.00 ± 0.07	0.72 ± 0.11***
P-SAPK/JNK	1.00 ± 0.06	0.97 ± 0.11	1.00 ± 0.13	0.99 ± 0.05
AKT	1.00 ± 0.03	0.98 ± 0.14	1.00 ± 0.06	1.14 ± 0.11
P-AKT (Ser473)	1.00 ± 0.13	0.95 ± 0.10	1.00 ± 0.14	0.85 ± 0.11
P-AKT (Thr308)	1.00 ± 0.18	0.68 ± 0.05*	1.00 ± 0.06	0.67 ± 0.17**

Lysates from E12.5 and E14.5 whole embryos were subjected to western blotting. For the quantification of phosphorylated protein levels, the ratios of phosphorylated protein to non-phosphorylated protein were determined by using ImageJ software and were then normalized to β-Actin. Intensity of non-phosphorylated proteins was normalized to β-Actin. Data are the means ± S.D. *, $P<0.05$, **, $P<0.01$, ***, $P<0.001$ vs. *Braf*$^{+/+}$; *Cre*.

Supplementary Table 2

MAPK protein levels of brain from embryos

	Brain	
	Braf$^{+/+}$; *Cre* (*n* = 5)	*Braf*$^{Q241R/+}$; *Cre* (*n* = 5)
BRAF	1.00 ± 0.20	1.24 ± 0.35
MEK	1.00 ± 0.05	1.06 ± 0.06
P-MEK	1.00 ± 0.21	1.32 ± 0.11*
ERK1/2	1.00 ± 0.04	1.02 ± 0.06
P-ERK1/2	1.00 ± 0.28	1.16 ± 0.13

Protein extracts obtained from the brains of E16.5 embryos were subjected to western blotting. Phosphorylated protein was measured to determine the ratios of phosphorylated protein to non-phosphorylated protein and normalized to β-Actin. Intensity of non-phosphorylated proteins was normalized to β-Actin. Data are the means ± S.D. *, $P<0.05$ vs. *Braf*$^{+/+}$; *Cre*.

Supplementary Table 3

Frequency of cardiac phenotypes in *Braf*$^{Q241R/+}$; *Cre* embryos at E16.5 (excluding edematous embryos)

Cardiac anomaly	No./Total	Percentage
VSD	2/14	14
Abnormal endocardial cushion	2/14	14
Enlarged		
PV	7/14	50
AV	3/14	21
TV	8/14	57
MV	9/14	64
Hypertrabeculation	3/14	21
Noncompaction	4/14	29
Epicardial blisters	2/14	14
Coronary artery hypoplasia	3/14	21

VSD, ventricular septal defect; PV, pulmonary valve; AV, aortic valve; TV, tricuspid valve; MV, mitral valve.

Supplementary Table 4

A list of cardiac phenotype in *Braf*$^{+/+}$; *Cre* and *Braf*$^{Q241R/+}$; *Cre* embryos at E16.5

Genotype	Ventricular septum	Valve	Trabecula and compact layer	Epicardium	Others
Braf$^{+/+}$; *Cre*-1					
Braf$^{Q241R/+}$; *Cre*-1		Enlarged PV, hypoplasia TV and MV	Hypertrabeculation of left and right ventricles	Epicardial blisters	
Braf$^{+/+}$; *Cre*-2					
Braf$^{Q241R/+}$; *Cre*-2		Enlarged TV and MV			Abnormal endocardial cushion
Braf$^{Q241R/+}$; *Cre*-3		Enlarged TV and MV			
Braf$^{+/+}$; *Cre*-3					
Braf$^{Q241R/+}$; *Cre*-4		Enlarged TV	Left ventricular noncompaction		
Braf$^{Q241R/+}$; *Cre*-5	Membranous VSD	Enlarged TV	Right ventricular noncompaction		
Braf$^{+/+}$; *Cre*-4					
Braf$^{+/+}$; *Cre*-5					
Braf$^{Q241R/+}$; *Cre*-6		Enlarged PV, AV, TV and MV	Hypertrabeculation of left and right ventricles, Left ventricular noncompaction		
Braf$^{+/+}$; *Cre*-6					
Braf$^{Q241R/+}$; *Cre*-7		Enlarged PV and TV	Left and right ventricular noncompaction		Abnormal endocardial cushion
Braf$^{Q241R/+}$; *Cre*-8		Enlarged PV		Epicardial blisters	Hypoplasia of coronary arteries
Braf$^{+/+}$; *Cre*-7					
Braf$^{Q241R/+}$; *Cre*-9		Enlarged PV, AV and MV			
Braf$^{+/+}$; *Cre*-8					
Braf$^{Q241R/+}$; *Cre*-10					
Braf$^{Q241R/+}$; *Cre*-11		Enlarged PV, AV, TV and MV	Hypertrabeculation of left and right ventricles		Hypoplasia of coronary arteries
Braf$^{Q241R/+}$; *Cre*-12		Enlarged MV			
Braf$^{+/+}$; *Cre*-9					
Braf$^{Q241R/+}$; *Cre*-13	Muscular VSD				
Braf$^{Q241R/+}$; *Cre*-14		Enlarged PV, TV and MV			Hypoplasia of coronary arteries

The thick frame represents littermates from a pregnant mouse. VSD, ventricular septal defect; PV, pulmonary valve; AV, aortic valve; MV, mitral valve; TV, tricuspid valve.

Supplementary Table 5

Probes used for Southern blotting

Probe	Sequence (5' to 3')
5' probe	Forward: CATCATACCCAGCAATAGTTTCAGT
	Reverse: TCAGCTGCTAATTCCTTATGATAGC
3' probe	Forward: ACAGTGTTCAGTAACTTGCCTACAG
	Reverse: ATACCTGCATATTGTGGACTCTTTC
Neo probe	Forward: GAACAAGATGGATTGCACGCAGGTTCTCCG
	Reverse: CGCCAAGCTCTTCAGCAATA

Supplementary Table 6

Primers used for genotyping

Gene	Sequence (5' to 3')
Braf	Forward: GTGTTGTTCTGCCCATACTTACTGC
	Reverse: GTGACTTAATGTACAGCATGGATCA
Cre	Forward: CTGATTTCGACCAGGTTCGTTC
	Reverse: CTAAGTGCCTTCTCTACACCTGC
Ptpn11	Forward: GACAGACCTGGTGGAGCATTAC
	Reverse: CAGCTTGCTTAACTCTCGAACC
Neo	Forward: GAACAAGATGGATTGCACGCAGGTTCTCCG
	Reverse: GTAGCCAACGCTATGTCCTGATAG

CLINICAL REPORT

AMERICAN JOURNAL OF medical genetics PART A

A Novel Heterozygous *MAP2K1* Mutation in a Patient with Noonan Syndrome with Multiple Lentigines

Eriko Nishi,[1,2] Seiji Mizuno,[3] Yuka Nanjo,[4] Tetsuya Niihori,[4] Yoshimitsu Fukushima,[2] Yoichi Matsubara,[4,5] Yoko Aoki,[4] and Tomoki Kosho[1,2]*

[1]Division of Medical Genetics, Nagano Children's Hospital, Azumino, Japan

[2]Department of Medical Genetics, Shinshu University School of Medicine, Matsumoto, Japan

[3]Department of Pediatrics, Central Hospital, Aichi Human Service Center, Kasugai, Japan

[4]Department of Medical Genetics, Tohoku University School of Medicine, Sendai, Japan

[5]National Research Institute for Child Health and Development, Tokyo

Manuscript Received: 31 March 2014; Manuscript Accepted: 1 October 2014

Noonan syndrome with multiple lentigines (NSML), formerly referred to as LEOPARD syndrome, is a rare autosomal-dominant condition, characterized by multiple lentigines, electrocardiographic conduction abnormalities, ocular hypertelorism, pulmonary stenosis, abnormal genitalia, growth retardation, and sensorineural deafness. To date, *PTPN11*, *RAF1*, and *BRAF* have been reported to be causal for NSML. We report on a 13-year-old Japanese boy, who was diagnosed with NSML. He was found to have a novel heterozygous missense variant (c.305A > G; p.E102G) in *MAP2K1*, a gene mostly causal for cardio-facio-cutaneous syndrome (CFCS). He manifested fetal macrosomia, and showed hypotonia and poor sucking in the neonatal period. He had mild developmental delay, and multiple lentigines appearing at approximately age 3 years, as well as flexion deformity of knees bilaterally, subtle facial characteristics including ocular hypertelorism, sensorineural hearing loss, and precocious puberty. He lacked congenital heart defects or hypertrophic cardiomyopathy, frequently observed in patients with NSML, mostly caused by *PTPN11* mutations. He also lacked congenital heart defects, characteristic facial features, or intellectual disability, frequently observed in those with CFCS caused by *MAP2K1* or *MAP2K2* mutations. This may be the first patient clinically diagnosed with NSML, caused by a mutation in *MAP2K1*.

Key words: Noonan syndrome with multiple lentigines (NSML); *MAP2K1*; cardio-facio-cutaneous syndrome (CFCS)

How to Cite this Article:
Nishi E, Mizuno S, Nanjo Y, Niihori T, Fukushima Y, Matsubara Y, Aoki Y, Kosho T. 2015. A novel heterozygous *MAP2K1* mutation in a patient with Noonan syndrome with multiple lentigines.
Am J Med Genet Part A 167A:407–411.

INTRODUCTION

Noonan syndrome with multiple lentigines (NSML), formerly referred to as LEOPARD syndrome, is a rare autosomal-dominant multiple congenital anomaly condition, characterized by multiple lentigines, electrocardiographic (ECG) abnormalities, ocular hypertelorism, pulmonary stenosis, genital abnormalities, growth retardation, and sensorineural deafness [Sarkozy et al., 2008; Gelb and Tartaglia, 2010; Martínez-Quintana and Rodríguez-González, 2012]. The diagnosis of NSML is made on clinical grounds by observation of specific features. Standard diagnostic criteria for NSML, proposed by Voron et al. [1976]; included multiple lentigines and two other cardinal features.

Together with Noonan syndrome (NS), Costello syndrome, cardio-facio-cutaneous syndrome (CFCS), and neurofibromatosis type 1, NSML is classified as RASopathy, a disorder affecting the RAS-MAPK signal transduction pathway [Aoki and Matsubara, 2013]. NSML is genetically heterogeneous and three causative genes have been identified, accounting for approximately 95% of affected individuals [Martínez-Quintana and Rodríguez-González, 2012]. Approximately 85% of patients with NSML have heterozygous

Conflict of interest: none.
Grant sponsor: Ministry of Health, Labour and Welfare, Japan; Grant sponsor: Nagano Children's Hospital Research Foundation.
*Correspondence to:
Tomoki Kosho, M.D., Department of Medical Genetics, Shinshu University School of Medicine, 3-1-1 Asahi, Matsumoto 390-8621, Japan.
E-mail: ktomoki@shinshu-u.ac.jp
Article first published online in Wiley Online Library (wileyonlinelibrary.com): 25 November 2014
DOI 10.1002/ajmg.a.36842

missense mutations in the protein-tyrosine phosphatase, non-receptor type 11 (*PTPN11*) gene (OMIM#151100). To date, 11 different *PTPN11* mutations, all localized in the protein-tyrosine phosphatase (PTP) domain, have been reported in NSML, two of which (p.T279C and p.T468M) constitute approximately 65% of the cases [Martínez-Quintana and Rodríguez-González, 2012]. Two unrelated patients with NSML were found to have heterozygous missense mutations in the v-Raf-1 murine leukemia viral oncogene homolog 1 (*RAF1*) gene (p.L613V and p.S257L) (OMIM#611554) [Pandit et al., 2007]. The p.L613V mutation increases kinase activity and enhances downstream ERK activation [Pandit et al., 2007]. Two unrelated patients with NSML had heterozygous missense mutations in the v-Raf murine sarcoma viral oncogene homolog B1 (*BRAF*) gene (p.T241P and p.L245F) (OMIM#613707) [Koudova et al., 2009; Sarkozy et al., 2009].

Mitogen-activated protein kinase 1 (MAP2K1) and MAP2K2 are dual-specificity protein kinases, which function as effectors of the serine/threonine kinase *RAF* family members by phosphorylating

FIG. 1. Clinical photographs of the patient at the age 7 months (A, B), at 2 5/12 years (C, D), and at 11 years (E–K).

and activating ERK proteins. A heterozygous missense mutation in *MAP2K1* is known to be causal for CFCS or NS [Allanson and Roberts, 2011; Rauen, 2012]. To date, all published *MAP2K1* mutations occurred in exons 2, 3, and 6.

In this report, we present a patient clinically diagnosed with NSML, who had a de novo novel and heterozygous *MAP2K1* variant with probable pathogenicity.

CLINICAL REPORT

The patient, a 13-year-old Japanese boy, was the second child of a healthy 30-year-old mother and a healthy 35-year-old nonconsanguineous father. His two brothers were healthy. He was born by normal vaginal delivery at 41 weeks and 4 days of gestation after an uncomplicated pregnancy. His birth weight was 4,350 g (+3.2 SD), length was 51 cm (+1.0 SD), and OFC was 37 cm (+2.6 SD). He showed hypotonia and sucked poorly in the neonatal period. He raised his head at age 3 months, rolled over at 4 months, and sat unsupported at 7 months. He showed no distinctive facial features and only a few lentigines in infancy (Fig. 1A, B).

His growth was impaired with a weight of 8.25 kg (−2.1 SD), height of 76.9 cm (−1.6 SD), and OFC of 45.6 cm (−1.4 SD) at age 1 7/12 years. His weight was 11 kg (−2.5 SD), height was 90.0 cm (−2.4 SD), and OFC was 49 cm (−0.4 SD) at age 2 10/12 years. Lentigines increased on the face and the limbs (Fig. 1C, D). He walked unassisted at age 3 3/12 years, and spoke a two-word sentence at 3 years. His intellectual quotient was 60 at 4 years, and 82 at 7 years. He showed growth acceleration from age 8.5 years, accompanied by a change in voice, and was diagnosed as precocious puberty at 9 years with an advanced bone age of 11.5 years. At age 10 years, his weight was 22.1 kg (−1.5 SD), height was 130 cm (−1.2 SD), and OFC was 51.8 cm (−1.0 SD). He underwent surgical elongation of his hamstrings, which reduced the limitation of bilateral knee extension from −60° degrees to −20° degrees.

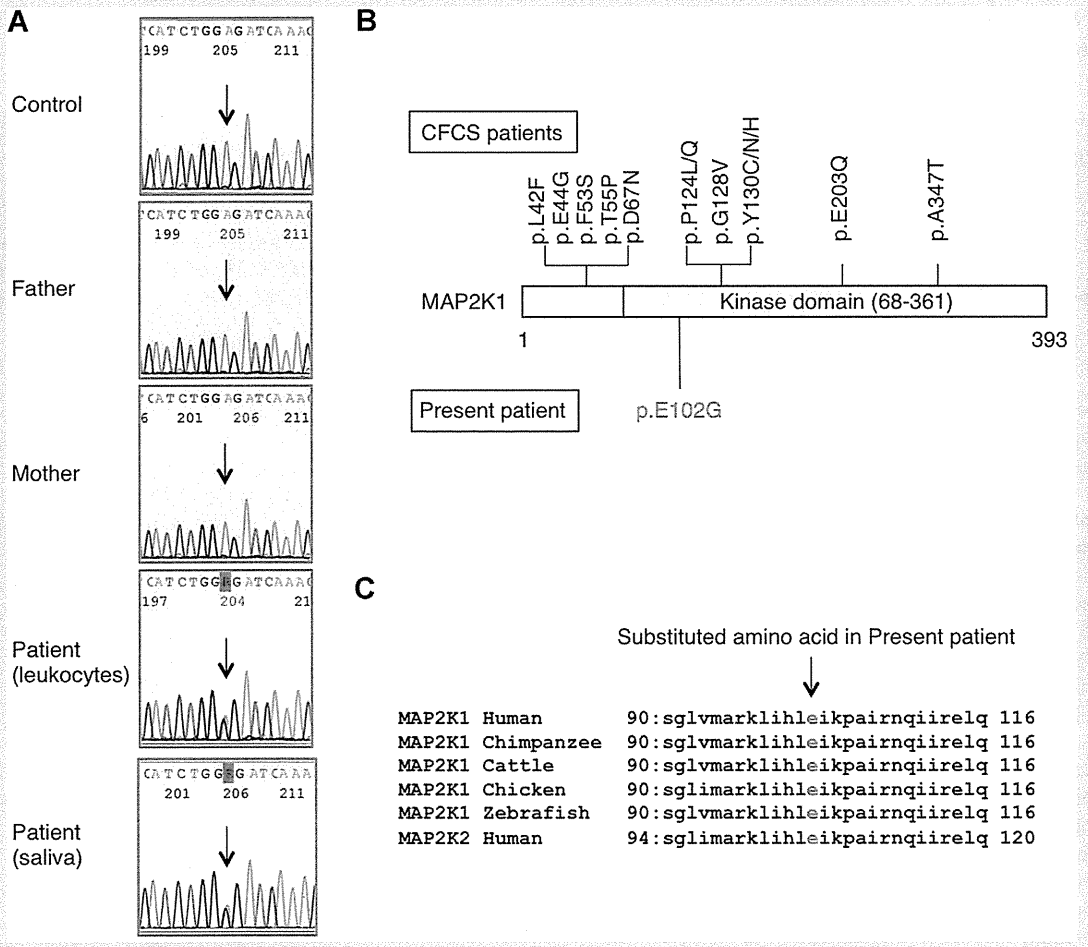

FIG. 2. A: Sanger sequencing of *MAP2K1*, showing an A→G substitution (c.305A > G, p.E102G) in exon 3, which was detected in the patient's DNA from leukocytes and saliva, but not detected in parental samples. B: MAP2K1 domain structure and location of residues altered in the present patient and previously reported patients with cardio-facio-cutaneous syndrome (CFCS). C: MAP2K1 amino acid alignment around the residue where the present amino acid change occurred. This residue is evolutionally conserved.

At age 11 years, his facial features included ocular hypertelorism, a long philtrum, thick upper and lower lip vermilions, and thickened ear helices (Fig. 1E, F). He had hyperextensible and dark skin with multiple lentigines all over the body, several café-au-lait spots, and fine wrinkles on the palms (Fig. 1G–J). He had a slender habitus with pectus carinatum, mild scoliosis, slender extremities, and limited extension of both elbows and knees (Fig. 1K). His weight was 23.0 kg (−1.8 SD) and height was 141 cm (−0.4 SD).

He had no abnormalities in the external genitalia. Resting or 24-hour ECG detected no conduction abnormalities. Echocardiography showed no congenital heart defects, pulmonary valve stenosis, or hypertrophic cardiomyopathy (HCM). Brain magnetic resonance imaging showed no structural abnormalities. He had bilateral mild sensorineural hearing loss with the threshold of 40 dB at approximately 2 kHz. G-banded chromosomes were normal.

MOLECULAR INVESTIGATION

Genomic DNA was isolated from the patient's leukocytes and saliva and his parents' leukocytes after appropriate informed consent. All coding exons and flanking introns in *PTPN11*, *KRAS*, *HRAS*, and *SOS1*, exons 6 and 11–16 in *BRAF*, exons 7, 14, and 17 in *RAF1*, exons 2 and 3 in *MAP2K1/2*, and exon 1 in *SHOC2* were amplified by polymerase chain reaction (PCR) with primers based on GenBank sequences. The primer sequences are available on request. PCR amplification was performed under standard condition using Taq DNA polymerase. After amplification, the PCR products were gel-purified and sequenced on the ABI 3500xL automated DNA sequencer (Applied Biosystems, Carlsbad, CA). A heterozygous missense variant (c.305A > G, p.E102G) was identified in exon 3 of *MAP2K1* in the patient's DNA extracted from his leukocytes and saliva. The variant was not detected in the parental samples (Fig. 2A). No mutation, other than c.305A > G in *MAP2K1*, was identified by the analysis using custom HaloPlex panel (Agilent Technologies, Santa Clara, CA) designed to identify mutations in exons and exon-intron boundaries of the following RASopathy-related genes: *PTPN11*, *HRAS*, *KRAS*, *NRAS*, *BRAF*, *RAF1*, *MAP2K1/2*, *SOS1*, *SHOC2*, *CBL*, *RIT1*, *NF1*, *SPRED1*, and *RRAS*.

DISCUSSION

The present patient had multiple lentigines, café-au-lait spots, ocular hypertelorism, growth impairment, sensorineural hearing loss, hypotonia, low average intelligence, and skeletal abnormalities.

TABLE I. Clinical Features of the Present Patient, Patients With Noonan Syndrome With Multiple Lentigines (NSML), and Patients With Cardio-Facio-Cutaneous Syndrome (CFCS) Caused by *MAP2K1* or *MAP2K2* Mutations

	Present patient	Patients with NSML [Gelb and Tartaglia, 2010]	Patients with CFCS caused by *MAP2K1* or *MAP2K2* mutations [Dentici et al., 2009]	
Causative gene	*MAP2K1*	*PTPN11* (90%) *RAF1* (n = 2) *BRAF* (n = 2)	*MAP2K1* (n = 41)	*MAP2K2* (n = 20)
Sex	Male	Male > Female	Male:Female = 9:14	
Nevi/lentigines	+	<100%	11/34 (32%)	
Café-au-lait spots	+	70–80%	5/30 (17%)	
Congenital heart defects	−	85%	25/39 (64%)	
HCM	−	70%	14/42 (33%)	
ECG abnormalities	−	23%	2/28 (7%)	
Pulmonary valve stenosis	−	25%	17/42 (40%)	
Polyhydramnios	−		20/32 (63%)	
Fetal macrosomia	+		13/25 (52%)	
Short stature	+	<50%	30/38 (79%)	
Macrocephaly	+		26/34 (76%)	
Hypertelorism	+		23/30 (77%)	
Thickened helix	+		27/30 (90%)	
Sparse hair	−		33/49 (67%)	
Sparse eyebrow	−		35/38 (92%)	
Palpebral ptosis	−		18/27 (67%)	
Flat nasal bridge	−		10/12 (83%)	
Joint limitation	+			
Failure to thrive	+		29/35 (83%)	
Intellectual disability	−	30%	43/46 (93%)	
Development delay	+		43/45 (96%)	
Hypotonia	+		40/45 (89%)	
Sensorineural hearing loss	+	<20%		
Seizures	−		16/44 (36%)	

CFCS, cardio-facio-cutaneous syndrome; ECG, electrocardiograph; HCM, hypertrophic cardiomyopathy , NSML, Noonan syndrome with multiple lentigines.

He lacked ECG conduction abnormalities, pulmonary stenosis, or abnormal genitalia. These findings were compatible with the standard diagnosis of NSML by Voron et al. [1976]. The variant c.305A > G, p.E102G was found de novo and not detected in db SNP Release 137 (http://www.ncbi.nlm.nih.gov/projects/SNP/), the Exome Sequencing Project (NHLBI-ESP) database (ESP6500SI-V2) (http://evs.gs.washington.edu/EVS/), the 1000 Genomes Project (1KGP) (http://www.1000genomes.org/), or the Human Gene Mutation Database (http://www.hgmd.cf.ac.uk/ac/index.php). In the COSMIC database, c.302_307delTGGAGA, resulting in an in-frame deletion (p.E102_I103delEI), has been identified in two samples with malignant melanoma and lung cancer (http://cancer.sanger.ac.uk/cancergenome/projects/cosmic/). The glutamine residue at codon 102 is located in the kinase domain (residues 68–361) of *MAP2A1* (Fig. 2B) and is conserved in higher organisms (Fig. 2C). Polymorphism Phenotyping v2 (PolyPhen-2) (http://genetics.bwh.harvard.edu/pph2/) predicts the variant to be possibly damaging, with a score of 0.711. In view of this evidence, the variant p.E102G may be causal for various clinical features consistent with NSML in the patient. However, no functional characterization of the variant was available and Sorting Intolerant From Tolerant (SIFT) (http://sift.jcvi.org) predicts the variant to be tolerated, with a score of 0.09.

We reviewed clinical features of the present patient, previously reported patients with NSML caused by *PTPN11* mutations in most (including two caused by *RAF1* mutations and two caused by *BRAF* mutations), and patients with CFCS caused by *MAP2K1* or *MAP2K2* mutations (Table I) [Pandit et al., 2007; Dentici et al., 2009; Koudova et al., 2009; Sarkozy et al., 2009]. Patients with NSML frequently had congenital heart defects and/or HCM, and sometimes had pulmonary valve stenosis and/or ECG abnormalities [Wakabayashi et al., 2011; Martínez-Quintana and Rodríguez-González, 2012], none of which were found in the present patient. Both patients with NSML caused by *RAF1* mutations had HCM, additionally, one had pulmonary valve stenosis, and the other had a mitral valve anomaly [Pandit et al., 2007]. One of the two patients with NSML caused by *BRAF* mutations had tetralogy of Fallot and the other had mitral and aortic valve dysplasia [Koudova et al., 2009; Sarkozy et al., 2009]. Patients with CFCS caused by *MAP2K1* or *MAP2K2* mutations frequently had congenital heart defects, polyhydramnios, characteristic facial "coarseness" (sparse hair/eyebrows, palpebral ptosis, and flat nasal bridge), and intellectual disability [Dentici et al., 2009], which were not found in the present patient. They rarely or sometimes had nevi, café-au-lait spots, or sensorineural hearing loss [Dentici et al., 2009], which were found in the present patient. Fetal macrosomia, postnatal failure to thrive/growth impairment, macrocephaly, hypotonia, developmental delay, and facial features including hypertelorism and thickened helices were shared by the present patient and over half of the patients with CFCS caused by *MAP2K1* or *MAP2K2* mutations.

In conclusion, the present patient may be the first to fit the standard clinical diagnostic criteria for NSML by Voron et al. [1976]; associated with a *MAP2K1* mutation. He lacked congenital heart defects or HCM, frequently observed in those with NSML, mostly caused by *PTPN11* mutations. He had fetal macrosomia, postnatal failure to thrive/growth impairment, macrocephaly, hypotonia, developmental delay, and hypertelorism but lacked congenital heart defect, characteristic facial features, or intellectual disability; which are frequently observed features in CFCS caused by *MAP2K1* or *MAP2K2* mutations. These observations could offer new insight into the phenotypic spectrum of RASopathies.

ACKNOWLEDGMENTS

We thank the patient and his parents for participating in this study. This work was supported by Research on Intractable Diseases from Ministry of Health, Labour and Welfare, Japan (Y.M., K.T.) and Nagano Children's Hospital Research Foundation (E.N.).

REFERENCES

Allanson JE, Roberts AE. 2011. Noonan syndrome. In: Pagon RA, Adam MP, Bird TD, et al., editors. GeneReviews® [Internet]. Seattle (WA): University of Washington; 1993–2014. Available from: http://www.ncbi.nlm.nih.gov/books/NBK1116/. Accessed March 16, 2014. .

Aoki Y, Matsubara Y. 2013. Ras/MAPK syndromes and childhood hemato-oncological diseases. Int J Hematology 97:30–36.

Dentici ML, Sarkozy A, Pantaleoni F, Carta C, Lepri F, Ferese R, Cordeddu V, Martinelli S, Briuglia S, Digilio MC, Zampino G, Tartaglia M, Dallapiccola B. 2009. Spectrum of MEK1 and MEK2 gene mutations in cardio-facio-cutaneous syndrome and genetype-phenotype correlations. Eur J Hum Genet 17:733–740.

Gelb BD, Tartaglia M. 2010. LEOPARD syndrome. In: Pagon RA, Adam MP, Bird TD, et al., editors. GeneReviews® [Internet]. Seattle (WA): University of Washington; 1993–2014. Available from: http://www.ncbi.nlm.nih.gov/books/NBK1116/. Accessed March 16, 2014. .

Koudova M, Seemanova E, Zenker M. 2009. Novel BRAF mutation in a patient with LEOPARD syndrome and normal intelligence. Eur J Med Genet. 52:337–340.

Martínez-Quintana E, Rodríguez-González F. 2012. LEOPARD syndrome: Clinical features and gene mutations. Mol Syndromol 3:145–157.

Pandit B, Sarkozy A, Pennacchio LA, Carta C, Oishi K, Martinelli S, Pogna EA, Schackwitz W, Ustaszewska A, Landstrom A, Bos JM, Ommen SR, Esposito G, Lepri F, Faul C, Mundel P, López Siguero JP, Tenconi R, Selicorni A, Rossi C, Mazzanti L, Torrente I, Marino B, Digilio MC, Zampino G, Ackerman MJ, Dallapiccola B, Tartaglia M, Gelb BD. 2007. Gain-of-function RAF1 mutations cause Noonan and LEOPARD syndromes with hypertrophic cardiomyopathy. Nat Genet 39:1007–1012.

Rauen KA. 2012. Cardiofaciocutaneous syndrome. In: Pagon RA, Adam MP, Bird TD, et al., editors. GeneReviews® [Internet]. Seattle (WA): University of Washington; 1993–2014. Available from: http://www.ncbi.nlm.nih.gov/books/NBK1116/. Accessed March 16, 2014. .

Sarkozy A, Digilio MC, Dallapiccola B. 2008. Leopard syndrome. Orphanet J Rare Dis 3:13.

Sarkozy A, Carta C, Moretti S, Zampino G, Digilio MC, Pantaleoni F, Scioletti AP, Esposito G, Cordeddu V, Lepri F, Petrangeli V, Dentici ML, Mancini GM, Selicorni A, Rossi C, Mazzanti L, Marino B, Ferrero GB, Silengo MC, Memo L, Stanzial F, Faravelli F, Stuppia L, Puxeddu E, Gelb BD, Dallapiccola B, Tartaglia M. 2009. Germline BRAF mutations in Noonan, LEOPARD, and cardiofaciocutaneous syndromes: Molecular diversity and associated phenotypic spectrum. Hum Mutat 30:695–702.

Voron DA, Hatfield HH, Kalkhoff RK. 1976. Multiple lentigines syndrome. Case report and review of the literature. Am J Med 60:447–456.

Wakabayashi Y, Yamazaki K, Narumi Y, Fuseya S, Horigome M, Wakui K, Fukushima Y, Matsubara Y, Aoki Y, Kosho T. 2011. Implantable cardioverter defibrillator for progressive hypertrophic cardiomyopathy in a patient with LEOPARD syndrome and a novel PTPN11 mutation Gln510His. Am J Med Genet A 155A:2529–2533.

RESEARCH ARTICLE

AMERICAN JOURNAL OF medical genetics PART A

Mutations in *PIGL* in a patient with Mabry syndrome

Ikuma Fujiwara,[1] Yoshiko Murakami,[2] Tetsuya Niihori,[3] Junko Kanno,[1] Akiko Hakoda,[1] Osamu Sakamoto,[1] Nobuhiko Okamoto,[4] Ryo Funayama,[5] Takeshi Nagashima,[5] Keiko Nakayama,[5] Taroh Kinoshita,[2] Shigeo Kure,[1] Yoichi Matsubara,[3,6] and Yoko Aoki[3]*

[1]Department of Pediatrics, Tohoku University School of Medicine, Sendai, Japan

[2]WPI Immunology Frontier Research Center and Research Institute for Microbial Diseases, Osaka University, Osaka, Japan

[3]Department of Medical Genetics, Tohoku University School of Medicine, Sendai, Japan

[4]Department of Medical Genetics, Osaka Medical Center and Research Institute for Maternal and Child Health, Izumi, Japan

[5]Division of Cell Proliferation, United Centers for Advanced Research and Translational Medicine, Tohoku University Graduate School of Medicine, Sendai, Japan

[6]National Research Institute for Child Health and Development, Tokyo, Japan

Manuscript Received: 10 June 2014; Manuscript Accepted: 8 December 2014

Mabry syndrome, hyperphosphatasia mental retardation syndrome (HPMRS), is an autosomal recessive disease characterized by increased serum levels of alkaline phosphatase (ALP), severe developmental delay, intellectual disability, and seizures. Recent studies have revealed mutations in *PIGV*, *PIGW*, *PIGO*, *PGAP2*, and *PGAP3* (genes that encode molecules of the glycosylphosphatidylinositol (GPI)-anchor biosynthesis pathway) in patients with HPMRS. We performed whole-exome sequencing of a patient with severe intellectual disability, distinctive facial appearance, fragile nails, and persistent increased serum levels of ALP. The result revealed a compound heterozygote with a 13-bp deletion in exon 1 (c.36_48del) and a two-base deletion in exon 2 (c.254_255del) in phosphatidylinositol glycan anchor, class L (*PIGL*) that caused frameshifts resulting in premature terminations. The 13-bp deletion was inherited from the father, and the two-base deletion was inherited from the mother. Expressing c.36_48del or c.254_255del cDNA with an HA-tag at the C- or N-terminus in *PIGL*-deficient CHO cells only partially restored the surface expression of GPI-anchored proteins (GPI-APs). Non-synonymous changes or frameshift mutations in *PIGL* have been identified in patients with CHIME syndrome, a rare autosomal recessive disorder characterized by colobomas, congenital heart defects, early onset migratory ichthyosiform dermatosis, intellectual disability, and ear abnormalities. Our patient did not have colobomas, congenital heart defects, or early onset migratory ichthyosiform dermatosis and hence was diagnosed with HPMRS, and not CHIME syndrome. These results suggest that frameshift mutations that result in premature termination in *PIGL* cause a phenotype that is consistent with HPMRS.

Key words: glycosylphosphatidylinositol anchor; Mabry syndrome; hyperphosphatasia mental retardation syndrome; genetic testing

How to Cite this Article:
Fujiwara I, Murakami Y, Niihori T, Kanno J, Hakoda A, Sakamoto O, Okamoto N, Funayama R, Nagashima T, Nakayama K, Kinoshita T, Kure S, Matsubara Y, Aoki Y. 2015. Mutations in *PIGL* in a patient with Mabry syndrome. Am J Med Genet Part A. 9999:1–9.

INTRODUCTION

In 1970, Mabry et al. reported three siblings with increased serum levels of alkaline phosphatase (ALP), severe developmental delay, intellectual disability, and seizures [Mabry et al., 1970]. Subsequently, a condition displaying the aforementioned symptoms was referred to as hyperphosphatasia with mental retardation (HPMR) syndrome or Mabry syndrome [Krawitz et al., 2010]. Other clinical features included distinctive facial features such as hypertelorism, a

Conflict of interest: none.
Grant sponsor: Biomedical Research Core of Tohoku University Graduate School of Medicine; Grant sponsor: Ministry of Health, Labor and Welfare of Japan; Grant sponsor: Japan Society for the Promotion of Science; Grant numbers: C: 25461535, C: 23590363; Grant sponsor: Takeda Science Foundation; Grant sponsor: Ministry of Education, Culture, Sports, Science, and Technology of Japan; Grant number: 25129705.
*Correspondence to:
Yoko Aoki, M.D., Ph.D, Department of Medical Genetics, Tohoku University School of Medicine, 1-1 Seiryo-machi, Sendai 980-8574, Japan. E-mail: aokiy@med.tohoku.ac.jp
Article first published online in Wiley Online Library (wileyonlinelibrary.com): 00 Month 2015
DOI 10.1002/ajmg.a.36987